JOURNAL OF APPLIED POLYMER SCIENCE VOL. 19, PP. 1037–1060 (1975)

The Effects of Melt History, Crystallization Pressure, and Crystallization Temperature on the Crystallization and Resultant Structure of Bulk Isotactic Polypropylene*

J. H. REINSHAGEN† and R. W. DUNLAP, *Department of Metallurgy & Materials Science, Carnegie-Mellon University, Schenley Park, Pittsburgh, Pennsylvania 15213*

Synopsis

A study of the effects of constant-pressure isothermal crystallization on polymer structure was conducted in bulk isotactic polypropylene. The investigation was designed to determine the influence of pressure, temperature, and melt history variables on the structure of this bulk polymer. Results demonstrate that the effects of pressure and crystallization temperature can be quite adequately combined into one processing parameter, undercooling (defined as the melting temperature minus the crystallization temperature), by use of the Clausius-Clapeyron equation. This parameter is demonstrated to be important in determining the kinetics of crystallization and the resultant structure. The moderate to high undercoolings involved in this study are representative of commercial injection-molding processes, and a number of conclusions regarding commercial processing are made based on these laboratory investigations.

INTRODUCTION

Macromolecular structure in polymers has been shown to be an important determinant of polymer physical properties, particularly those properties associated with mechanical deformation.[1–10] Since macromolecular structure itself is influenced primarily by thermal processing, understanding the relationship between structural and processing variables is an important step in rationalizing and ultimately optimizing polymer properties.

The basic processing variables which control polymer crystallization and resultant structure, both in commercial processes and more controlled laboratory experiments, are temperature and pressure. In a commercial process such as injection molding, the polymer melt at some fixed temperature is injected at a fixed injection pressure into a mold at a lower set temperature. Following injection, both temperature and pressure of the polymer melt decrease with time in a manner determined by the mold temperature, injection temperature and pressure, and machine-mold design. An investigation of the effects of temperature

* This paper is part of a dissertation submitted by J. H. Reinshagen to the Department of Metallurgy and Materials Science, Carnegie-Mellon University, in partial fulfillment of the requirements for the degree of Doctor of Philosophy.

† Present address: Bettis Atomic Power Laboratory, Westinghouse Electric Corporation, P. O. Box 79, West Mifflin, Pennsylvania 15122.

and pressure on crystallization and resultant structure in commercially processed polymers can be severely limited by highly variable machine-mold characteristics. To eliminate machine-mold effects in this study and still determine the effects of other processing conditions, the idealized case of isothermal crystallization under constant pressure was employed.

In the course of this investigation it was determined that undercooling, defined as the melting temperature minus the crystallization temperature and calculated with the aid of the Clausius-Clapeyron equation, was an excellent parameter for interrelating crystallization temperature and pressure. This is not the first study to apply the Clausius-Clapeyron equation to polymer systems. Over the course of several decades, however, its use has generally been limited to determination of thermodynamic properties at the melting "temperature" of various polymer systems.[11-14] Martin and Mandelkern[15] studied isothermal crystallization of natural rubber at several pressures and used the Clausius-Clapeyron equation to determine the pressure dependence of the melting point, but did not identify the full significance of the undercooling parameter. Wunderlich and Arakawa[16] used pressure to vary the melting temperature of polyethylene and, by appropriately varying crystallization temperature, studied pressure effects at constant undercooling.

Limited studies of the influence of undercooling varied by variation of crystallization temperature have been previously reported.[17,18] The results reported here are unique in that the undercooling variable is demonstrated to be a convenient tool for studying the combined effects of pressure and crystallization temperature on crystallization and resultant structure. A principal advantage of this technique is that it facilitates the comparison of pressure–temperature effects under processing conditions that simulate commercial practice.

EXPERIMENTAL PROCEDURE AND BASES FOR DATA ANALYSIS

Polymer

The polymer used in this study was Hercules Profax 6623, a commercially available, general-purpose, heat-stabilized polypropylene. The polymer was characterized by Hercules as having a $M_w = 418{,}000$, a $M_n = 61{,}000$, an intrinsic viscosity of 2.7 dl/g (Decalin 135°C), and a nonisotactic (Decalin solubles) content of about 3%.

Molding Rig

The constant-pressure molding rig employed in this study was capable of pressures up to 13,000 psi. The rig was inserted in the melt bath (at a temperature between 190° and 220°C) for isothermal melt treatment and then transferred to the crystallization bath for isothermal crystallization at a temperature between 120° and 150°C. The finished samples were in the form of rods about $^5/_{16}$ in. in diameter and $2^1/_2$ in. long. The molding rig and molding procedure employed in this study are more fully described elsewhere.[19]

Density Determination

Densities were determined in a 1-propanol–water density gradient column at 23.00 ± 0.01°C. The 70-cm column had a working range from about 0.896 to

0.921 g/cm^3 and a density gradient of about 4×10^{-4} g/cm^3 per centimeter of column, which allowed densities to be easily read to four decimal places.

X-Ray Studies

X-Ray diffraction patterns were obtained from representative samples using the Debye-Scherrer method, copper K_α radiation, a 11.46-cm-diameter Debye camera, and 6-hr exposures.

Determination of Spherulite Diameter and Nucleation Density

Spherulite diameter was determined via lineal analysis,[20] using polished and heat etched samples, by reflected light microscopy. The spherulite diameter thus determined is simply the inverse of the average number of spherulite boundaries intersected per unit length by random straight lines projected on the sample surface.

Nucleation density was then calculated from spherulite diameter assuming predetermined nucleation[21] (i.e., all nuclei are assumed present and active from the start of crystallization, or very shortly thereafter) and the relation[20]

$$N_v \simeq (3/4D)^3$$

where N_v is the nucleation density and D is the spherulite diameter. (A complete listing of symbols used in the text is provided in Appendix I.) This relation is most frequently employed to determine nucleation density from grain diameter in metals. It is based on the assumption that all spherulites are of equal size, which optical microscopy confirmed to be approximately the case for the samples studied.

Dilatometry

Dilatometric data were obtained using a dial gauge micrometer mounted atop the ram of the molding rig.

Figure 1 shows a typical dilatometric trace, here for an undercooling of 63.2°C. Time zero corresponds to the time the rig is inserted in the crystallization bath following melt treatment. At undercoolings smaller than 63.2°C, the inflection point that occurs on Figure 1 at about 5 min appears more as a level plateau, while at larger undercoolings the inflection is less pronounced.

Determination of Specific Volume Change on Fusion

As shown in Figure 1, Δh is the height change due to contraction of the melt on cooling from the melt temperature T_m to the crystallization temperature T_x; Δh is readily determined at small undercoolings where the level plateau is seen on the dilatometric trace. There, it is simply the difference between the sample height at insertion into the melt bath and the sample height that corresponds to the level plateau. For larger undercoolings such as that represented on Figure 1, Δh was determined empirically by extrapolation of the small undercooling data.

It was not possible to accurately measure the final height of the polymer sample under pressure at the crystallization temperature, so the polymer was arbitrarily assumed to be fully crystallized when

$$\frac{(dh/dt)}{h_{RT}} = 1.5 \times 10^{-4}\ \text{min}^{-1}$$

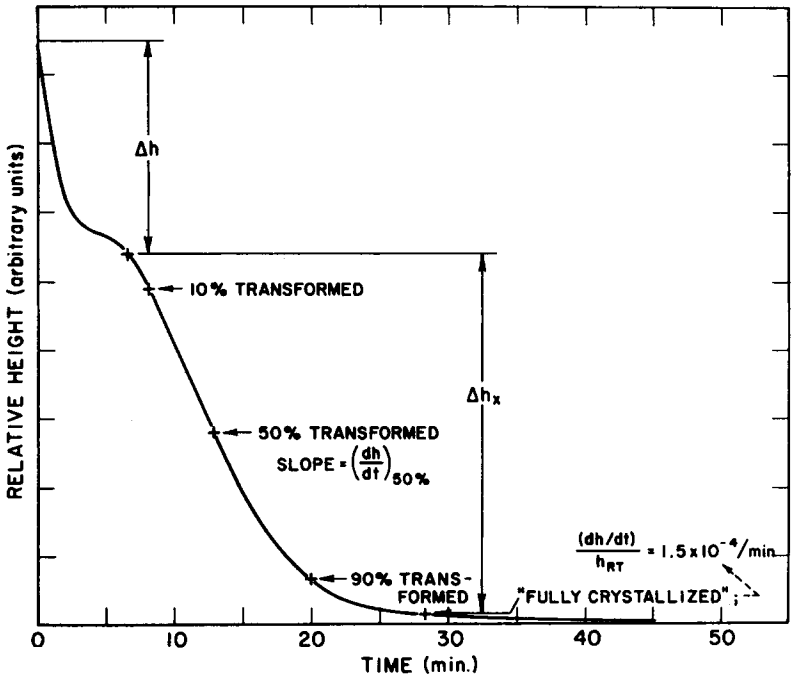

Fig. 1. Typical dilatometric trace.

with h_{RT} being the room-temperature sample height. As seen on Figure 1, this condition is met in the early portion of the long tail of the dilatometric trace, a region which is characteristic of both volumetric creep and the final stages of crystallization, frequently referred to as secondary crystallization. Note again that the choice of the value for $(dh/dt)/h_{RT}$ is arbitrary. Any value that corresponds to the early portion of the tail of the dilatometric trace would be equally suitable and yield similar results.

Thus, to obtain Δh_x, the height change of the sample due to crystallization, Δh is subtracted from the total height change that occurs between insertion in the crystallization bath and the attainment of the fully crystallized state. The specific volume change on fusion of the whole polymer, ΔV_f, is simply

$$\Delta V_f = \frac{\pi R^2 \Delta h_x}{M_0}$$

where R is the cylindrical mold radius and M_0 is the sample mass. Empirically it was found that the equation

$$\Delta V_f(\text{cm}^3/\text{g}) = -6.39 \times 10^{-4} T_x(^\circ\text{K}) + 2.18 \times 10^{-6} P\ (\text{psi}) + 1.69 \times 10^{-1} \quad (1)$$

predicted values of ΔV_f within 10% of the experimentally determined volume change, P being the crystallization pressure.

Determination of Times for 10, 50, and 90 Mass Per Cent Transformed

The volume change dV that results when an amount of polymer of mass dM is transformed from the amorphous to the semicrystalline state is simply

$$dV = (V_a - V_{sc})dM$$

where V_a is the specific volume of the amorphous melt and V_{sc} is that of the semicrystalline polymer. Due to the cylindrical geometry of the mold employed, note that

$$dV = \pi R^2 dh$$

where R is the mold radius and dh is the change in sample height due to the volume change dV. It follows that

$$dM = \frac{\pi R^2}{(V_a - V_{sc})} dh.$$

Thus, since π, R, V_a, and V_{sc} are constant, the amount of mass transformed is simply proportional to the change in sample height. Since full transformation of the sample corresponds to a height change of Δh_x, it is evident that the states of 10, 50, and 90 mass-% transformed correspond to height changes of 10%, 50%, and 90% of Δh_x, respectively.

Times required for 10, 50 and 90 mass-% transformed then follow directly from the dilatometric traces.

Determination of Spherulite Radial Growth Rate

As detailed in Appendix II, spherulite radial growth rates at 50 mass-% transformed, $(dr/dt)_{50\%}$, may be calculated from the time rate of change of sample height at 50 mass-% transformed, $(dh/dt)_{50\%}$, and the final spherulite diameter D. The analysis shows that

$$(dr/dt)_{50\%} = \frac{0.44D}{\Delta h_x} (dh/dt)_{50\%}.$$

Differential Scanning Calorimetry

DSC investigations were conducted using a Perkin-Elmer differential scanning calorimeter employing a heating rate of 10°C/min. DSC samples, cut from the molded specimens with a scalpel, weighed between 2 mg and 10 mg.

Determination of Heat of Fusion

Heats of fusion (really heats of melting) were determined from the areas under the DSC traces after calibration with an indium sample. For the whole polymer, it was empirically determined that

$$\Delta H_f(\text{cal/g}) = -9.15 \times 10^{-2} T_x(°\text{K}) + 15.71 \quad (2)$$

for samples crystallized at 3768 psi. (There were not sufficient data to determine the pressure dependence of ΔH_f.)

Determination of Melting Temperature and Lamellar Thickness

The melting temperature of a particular sample measured at atmospheric pressure, T'_{mp}, was chosen as the temperature corresponding to the maximum of the major DSC peak. This is representative of the temperature at which the greatest number of lamellae melt. For samples crystallized under a pressure of 3768 psi it was determined that

$$T'_{mp}(°\text{K}) = 3.18 \times 10^{-1} T_x(°\text{K}) + 308.3. \quad (3)$$

Lamellar thickness l was determined from T'_{mp} using an empirical equation developed from the data of Blais and Manley.[22] These investigators used small-

angle x-ray scattering to determine l in a polypropylene of molecular weight and distribution quite similar to that of the polymer used in this study. The relationship

$$l(\text{Å}) = \frac{14.4}{\left[1.04 - \frac{T'_{mp}(°\text{K})}{T^{\infty}_{mp}(°\text{K})}\right]}$$

was used where T^{∞}_{mp} corresponds to the melting point of a lamella of infinite extent and T'_{mp}, as determined above, corresponds to the melting point of a lamella of thickness l much less than lateral dimensions. As outlined later, T^{∞}_{mp} was chosen as 458°K, the equilibrium melting point at one atmosphere pressure (zero molding pressure).

Determination of the Undercooling Parameter

Undercooling is defined as $\Delta T = T_{mp} - T_x$, where T_x is the crystallization temperature and T_{mp} is the equilibrium melting temperature. The effect of pressure on the melting temperature is determined from the Clausius-Clapeyron equation, which may be written

$$T_{mp} = \left[\frac{\Delta V_f T^0_{mp}}{\Delta H_f}\right](P - P_0) + T^0_{mp}$$

where T^0_{mp} is the equilibrium melting temperature at the reference pressure P_0; and T_{mp}, the melting temperature employed in the undercooling equation, is the equilibrium melting temperature at pressure P. The reference pressure was chosen as the molding pressure most commonly employed, 3768 psi.

The commonly employed procedure for determining the equilibrium melting temperature in polymer systems is to take the temperature at which the extrapolation of a plot of measured melting temperature versus crystallization temperature intersects the line for which measured melting temperature equals crystallization temperature.[23] Presumably this is the temperature at which crystallization would occur at an infinitely slow rate. The procedure is quite straightforward if the samples are crystallized under the same pressure as that at which their melting temperature is measured. Since this not the case for the samples employed in this study, and since pressure does influence measured melting temperature, a slightly more complex procedure is required. This procedure is illustrated in Figure 2.

The data points shown on this figure represent the measured DSC melting temperature T'_{mp}, plotted as a function of crystallization temperature, and fit with a least-squares line. Note the very important distinction that, although the samples represented by these data points were crystallized under a pressure of 3768 psi, T'_{mp} is measured at atmospheric pressure ($P = 0$), not at 3768 psi. As outlined in Appendix III, T''_{mp} represents the value of T'_{mp} that would be obtained if the samples had been melted at the reference pressure of 3768 psi. This procedure is necessary to reference the melting temperature to the same pressure under which the samples were crystallized (i.e., 3768 psi). Thus, T^0_{mp} is chosen as the temperature at which the T''_{mp} line intersects the line defined by $T''_{mp} = T_x$. This procedure yields a value of $T^0_{mp} = 471.3$°K.

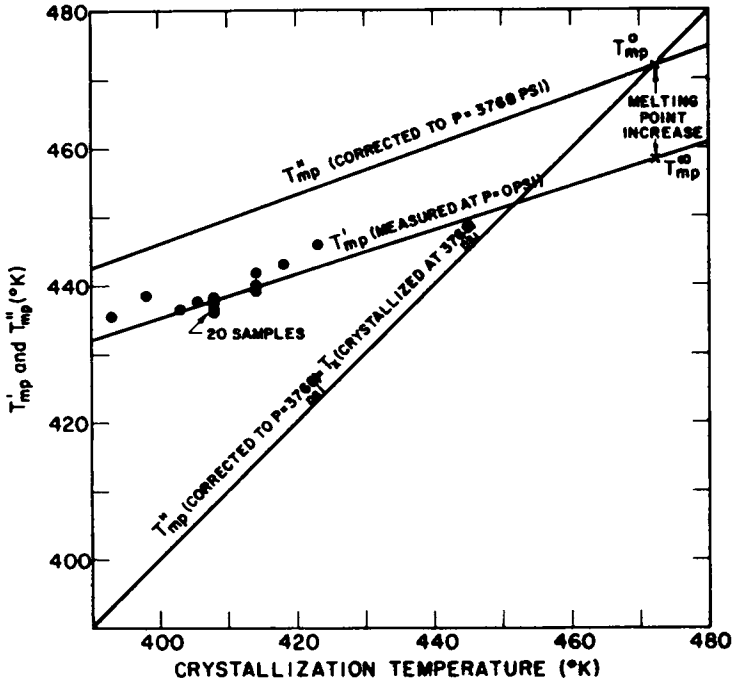

Fig. 2. Determination of T^0_{mp} (see text).

The melting point at atmospheric pressure of a crystal of infinite extent, T^∞_{mp}, used in the lamellar thickness equation, is then determined as the value T^0_{mp} would have at atmospheric pressure ($P = 0$). Graphically, this corresponds to subtracting the distance marked "melting point increase" from T^0_{mp}, as shown on Figure 2. A value of $T^\infty_{mp} = 458.0°\text{K}$ was determined.

Once T^0_{mp} is known, values of ΔH_f and ΔV_f at T^0_{mp} and the reference pressure follow directly by substitution of $T_x = T^0_{mp}$ in eqs. (1) and (2).

To summarize, at the reference pressure of 3768 psi we find

$$T^0_{mp} = 471.3 \pm 3.6°\text{K}$$

$$\Delta V_f = -0.124 \pm 0.008 \text{ cm}^3/\text{g}$$

$$\Delta H_f = -27.4 \pm 2.4 \text{ cal/g}.$$

For use in the Clausius-Clapeyron equation, the accuracy of the calculation can be increased by taking into account the pressure dependence of ΔV_f, as shown by eq. (1). A summary of calculated undercoolings for the experimental conditions employed in this study are shown in Table I.

RESULTS AND DISCUSSION

The discussion of experimental results is arranged for convenience into three sections: (1) a discussion of the effect of undercooling and melt treatment on the kinetics of crystallization; (2) an elucidation of the influence of these variables on resultant polymer structure; (3) a discussion of the application of these results to commercial processing.

TABLE I
Summary of Experimental Conditions

T_x, °C	P, psi	T_{mp}, °C	ΔT, °C
150	3768	198.2	48.2
145	3768	198.2	53.2
135	1641	190.4	55.4
140.9	3768	198.2	57.3
140.6	3768	198.2	57.6
135	3171	196.1	61.1
135	3768	198.2	63.2
140.9	6273	206.6	65.7
132.5	3768	198.2	65.7
130	3768	198.2	68.2
135	5925	205.5	70.5
125	3768	198.2	73.2
135	8066	212.2	77.2
120	3768	198.2	78.2
140.9	12573	224.4	83.5

Kinetic Effects

Figure 3 is a time–temperature–transformation (TTT) curve compiled from dilatometric traces such as the one shown in Figure 1. The plot illustrates the times required to reach states of 10, 50, and 90 mass-% transformed for a given undercooling. The data for variations in crystallization temperature fit quite well with the data for variations in pressure, indicating the applicability of the Clausius-Clapeyron equation for relating the two. Note that data for this figure, as well as data for several succeeding figures, correspond to samples given three different melt treatments: 11 min at 195°C, 11 min at 200°C, and 30 min at

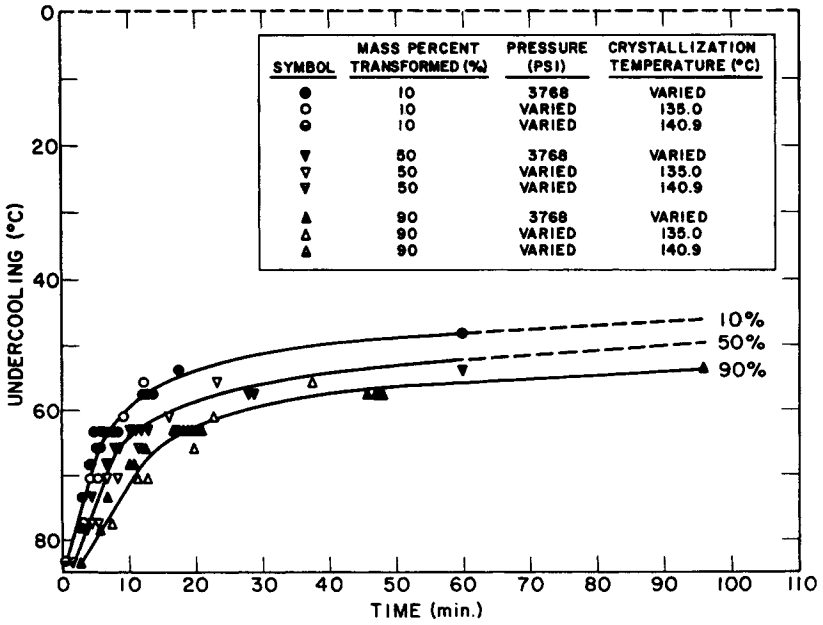

Fig. 3. TTT Illustrating 10, 50, and 90 mass-% transformed for moderate melt treatment.

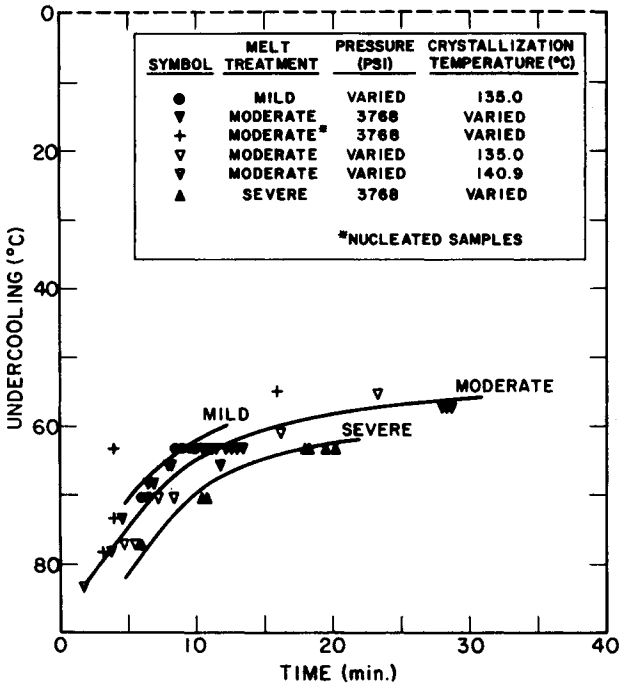

Fig. 4. TTT illustrating effect of melt history.

200°C. These melt treatments, termed "moderate," were sufficiently similar so that data could be combined with negligible effect on accuracy.

Note that at small undercoolings crystallization time is very large, a result of both fewer nuclei and slower spherulite growth rates under these conditions. For example, an increase in undercooling from 60° to 80°C results in a fivefold decrease in time needed for 50% crystallization. To achieve rapid crystallization consonant with rapid production rates, a commercial processor operates in the region of greater undercooling, producing these conditions by increased crystallization pressure and/or decreased mold temperature.

Figure 4 compares the 50 mass-% transformed line for the three combined "moderate" melt treatments shown on Figure 3 with that for a "mild" melt treatment (11 min at 190°C) and a "severe" melt treatment (120 min at 220°C). Note the ability of decreasing severity of melt treatment to also decrease crystallization time at set undercooling. This is because increased severity of melt treatment results in increased deactivation of nuclei and thus fewer crystallization centers are active at the crystallization temperature. Thus, to achieve the more rapid crystallization desirable in commercial processes, mild melt treatments are in order.

Often nucleating agents are also used for this same purpose. To compare the effects of nucleating agents with melt treatment, small amounts of a nucleating agent (either sodium benzoate or indigo) were added to four samples that were then given a moderate melt treatment. As seen on Figure 4, although in all cases the time to 50% crystallization was reduced, higher undercoolings produce sufficient undercooling induced nuclei to be as effective as addition of a nucleating agent. A more quantitative discussion is not possible because, in these trial runs,

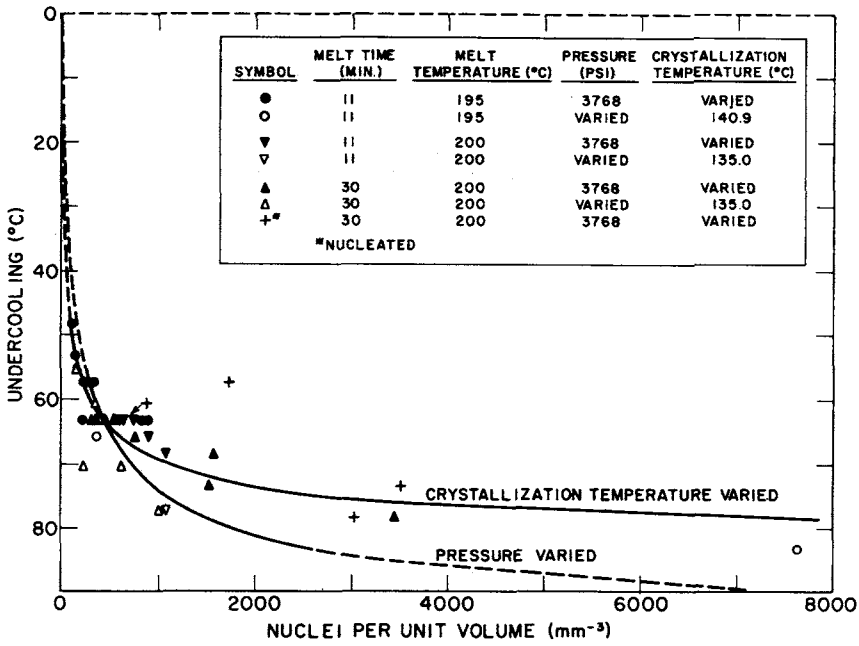

Fig. 5. Effect of undercooling on nucleation density for moderate melt treatment.

the type or the amount of nucleating agent added was not constant, and because distribution of the agent is quite likely very non-uniform.

The effect of undercooling on nucleation density (predetermined nucleation assumed) is illustrated in Figure 5. The four nucleated samples are also shown. In this case, data from varied pressure and varied crystallization temperature do not combine well. An explanation of this effect may be found from the work of Rybnikar,[24] who pointed out that minute gas or vapor pores act as nuclei in polypropylene. It seems reasonable that increased pressure has the effect of closing some of these pores, or at least making them too small to act as effective nuclei. Hence, an increase in undercooling due to a decrease in crystallization temperature at constant pressure is somewhat more effective in increasing nucleation density than is an identical increase in undercooling due to an increase in pressure at constant crystallization temperature. The difference is small, and although apparent when directly plotted as in Figure 5, is not evident on the TTT plots.

In contrast to commercial practice, the samples involved in this study were held under vacuum during much of the melt treatment. Thus, the effect demonstrated here should be more pronounced in commercial processing where more gas entrapment occurs.

Figure 6 shows the effect of mild, moderate, and severe melt treatments on nucleation density for undercooling varied by pressure variation at constant crystallization temperature. Here, the ability of increasing severity of melt treatment to deactivate nuclei is clearly demonstrated.

Figure 7 shows how undercooling affects spherulite radial growth rate measured at 50 mass-% crystallized. (Data are not differentiated by melt treatment since this variable has no influence on growth rate.) Growth rate is determined by two factors: the diffusion rate of the polymer chains through the melt, which

decreases with increasing ΔT; and the nucleation rate of the polymer chains on the growth faces of the crystalline lamellae, which increases with increasing ΔT. The data shown in Figure 7 are in the undercooling region where the nucleation event is controlling. The Clausius-Clapeyron equation is seen to combine the

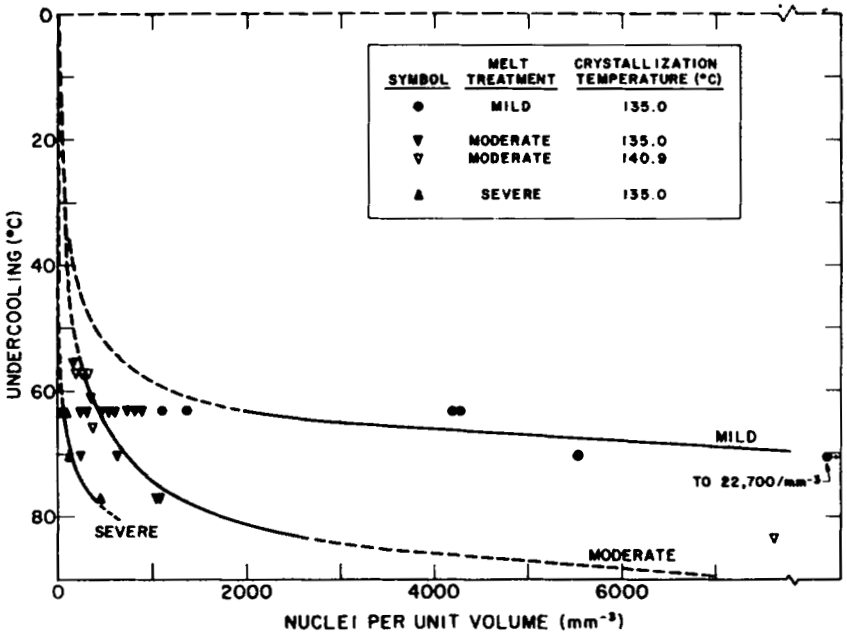

Fig. 6. Effect of undercooling and melt history on nucleation density: pressure varied.

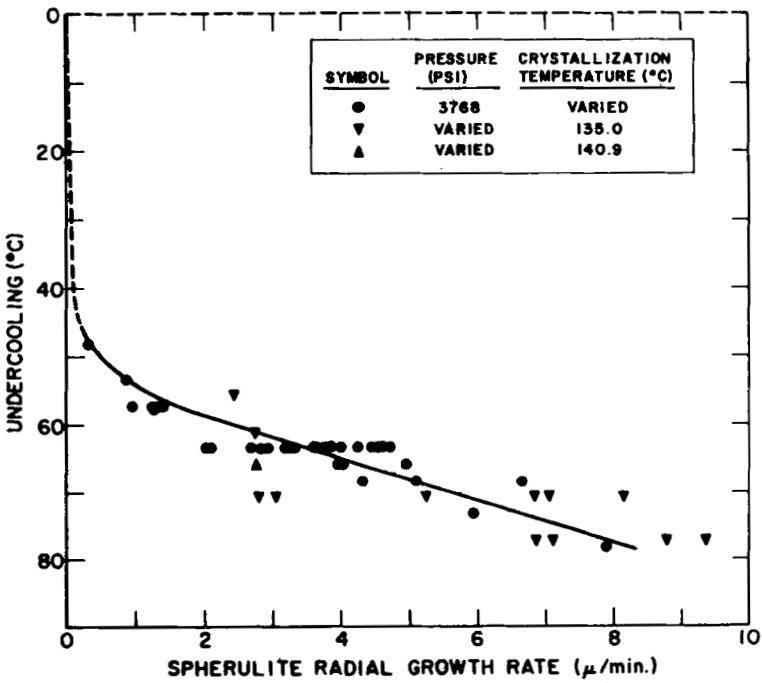

Fig. 7. Effect of undercooling on spherulite growth rate.

data quite adequately. Note that growth rate and nucleation density combine to give the overall crystallization rate (Figs. 3 and 4).

Resultant Structure

Having illustrated the effects of undercooling and melt treatment on the kinetics of the transformation, the influence of these variables on resultant polymer structure can now be explained.

Spherulite Diameter

Figure 8 shows the effect of undercooling on spherulite diameter for moderate melt treatment. As with the nucleation density results, the Clausius-Clapeyron equation does not quite adequately combine pressure and temperature variations, and these variations are differentiated on the figure. Least-squares lines for pressure and temperature induced variations are shown, along with 90% confidence bands for these lines. Note that the confidence bands do just overlap, a further indication that the differences between pressure variation data and crystallization temperature variation data are small. Note the nucleated samples are also illustrated.

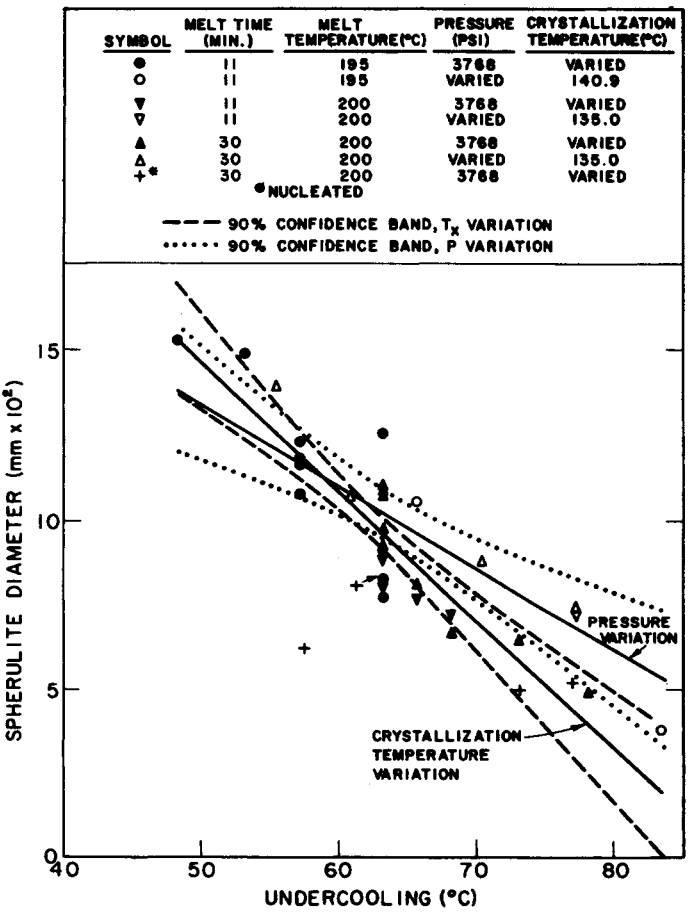

Fig. 8. Effect of undercooling on spherulite diameter for moderate melt treatment.

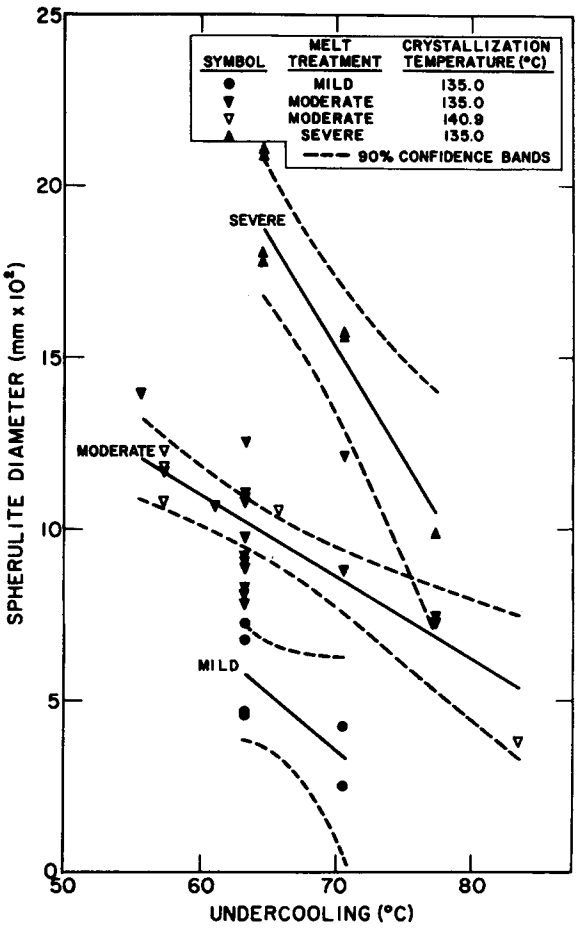

Fig. 9. Effect of undercooling and melt history on spherulite diameter: pressure varied.

Figure 9 illustrates the effect of mild, moderate, and severe melt treatments on spherulite diameter for undercooling varied by pressure. The 90% confidence bands for least-squares lines representing each melt treatment are illustrated. All lines can be drawn with the same slope and still easily remain within their respective confidence bands, illustrating the uniformity of the undercooling effect.

To achieve minimum spherulite diameter (for example, for maximum optical clarity), a mild melt treatment (low melt temperature) would be used in combination with high undercooling (high pressure and low crystallization temperature). As seen from Figure 8 (where moderate melt treatment results are illustrated), this combination would produce a spherulite diameter at least as small as that found for any of the nucleated samples, while eliminating the problem of even distribution of the nucleating agent. Note, however, there are practical limitations that govern the undercooling that may be achieved. For example, heat flow considerations may limit the minimum crystallization temperature obtainable. High pressure may cause excessive flash and mold abrasion. Use of a nucleating agent would eliminate these problems by allowing operation at lower undercooling while still providing a small spherulite size and the fast crystallization kinetics required for short cycles.

For an undercooling of about 65°C, a change in melt treatment from moderate to mild (roughly equivalent to a 10°C decrease in melt temperature) results in halving the spherulite diameter. To achieve the same results for a moderate melt treatment, an undercooling increase of about 20°C is required.

Density

Figure 10 is a plot of density as a function of undercooling. With the exception of the two data points at the highest undercooling, to be discussed later, the relationship appears quite linear, and a least-squares line with a 90% confidence band is used to illustrate the data. The plot shows decreasing density with increasing undercooling. There are three possible reasons for this effect: (1) a change in the crystal structure of the polymer (or a change in the relative amounts of two crystalline phases present); (2) a change in void content; and (3) a change in per cent crystallinity. A change in per cent crystallinity is the generally accepted reason for a change in density with undercooling.[25]

To check if the change in density could be due to varying amounts of different crystalline phases, x-ray diffraction patterns were obtained for representative samples. The x-ray results revealed that all samples contained both α and γ crystals. (Diffraction patterns from untreated, as received pellets showed only α crystals.) With the exception of the two samples crystallized at the highest

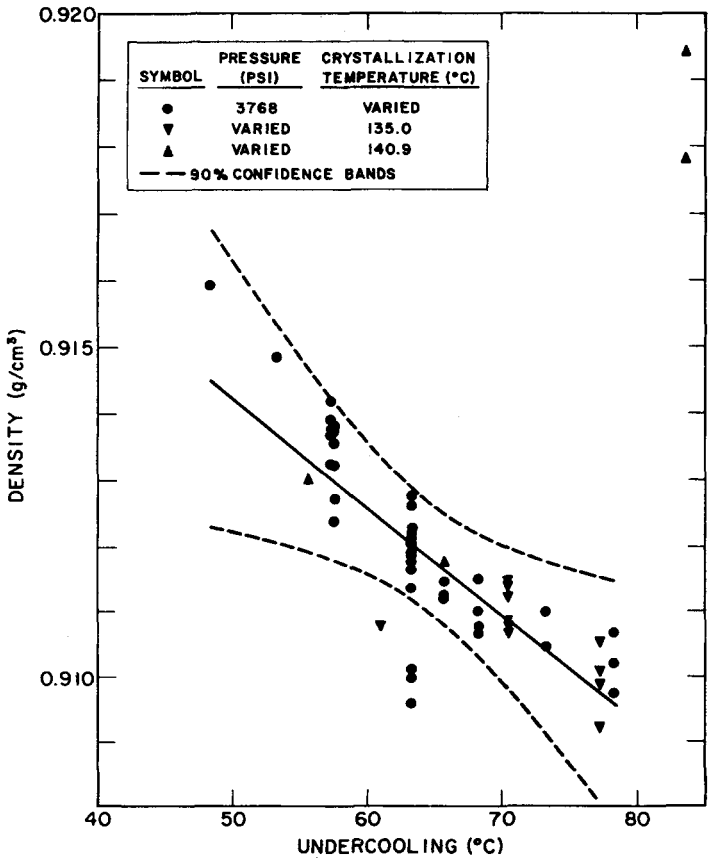

Fig. 10. Effect of undercooling on density.

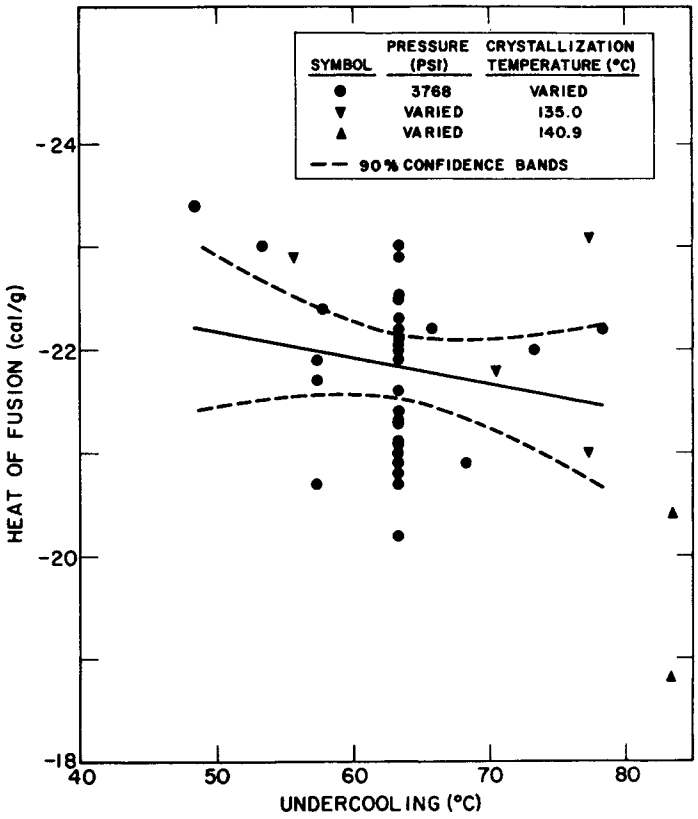

Fig. 11. Effect of undercooling on heat of fusion.

undercooling employed, all samples uniformly had about five times as much α as γ. We estimate this α to γ ratio to be accurate and constant to at least $\pm 40\%$. The density of 100% crystalline α is 0.936 g/cm^3,[26] while that of γ is between 0.945 g/cm^3 and 0.950 g/cm^3.[27] The density of amorphous material is 0.850 g/cm^3.[26]

Using the higher estimate for the γ density, a polymer with 70 vol-% crystallites made up (by volume) of five times as much α as γ would have a density of 0.9118 $\pm$ 0.0006 g/cm^3, the variability being determined by the 40% figure quoted above. This density is typical of the densities measured in this study. Thus, for a constant per cent crystallinity, variation of the relative amounts of α and γ within the estimated limits could account for only a small amount (0.0012 g/cm^3, equal to twice the ± 0.0006 g/cm^3 figure) of the density variation shown in Figure 10. Thus, the effect is not due to the variation of the relative amounts of the crystalline phases present.

DSC heat of fusion measurements were made on representative samples with the hope of comparing these results with the density results to get a measure of how void content might change with undercooling. This is possible because density percent crystallinity is affected by a change in void content while heat of fusion per cent crystallinity is not. (Note a change from zero to 10% void volume would result in a nearly 10% decrease in density, a figure which is greater than the range of change in density with undercooling illustrated in Fig. 10.) Figure 11 is a plot of the heat of fusion measurements as a function of undercool-

ing. (This variable was chosen rather than per cent crystallinity because of the presence of both α and γ.) The 90% confidence band of the least-squares line is illustrated. The two highest undercooling data points, which were omitted from the least-squares calculation, will be discussed later. Note the considerable scatter, probably the result of: (1) the difficulty encountered in cutting DSC samples without deformation; (2) the problem of accurately drawing the baseline tangent to the low-temperature end of the DSC trace; (3) planimeter error. This scatter makes a meaningful quantitative comparison of density and heat of fusion data impossible.

The results of optical microscopy are of help in resolving the issue. Samples crystallized at the smallest undercoolings employed showed crack or void networks at the spherulite boundaries, a phenomenon not apparent in samples crystallized at higher undercoolings. Note, however, that the small undercooling samples have the highest densities, opposite the trend expected if they have higher void content. Hence, if void content is changing, the change is small enough to be overshadowed by other effects.

It follows that the change in density with undercooling is primarily due to a change in percent crystallinity. This is presumably because lamellae formed at high growth rates (associated with large undercoolings) are less perfect due to faster nucleation of polymer chains on the growth faces of the lamellae and shorter times available for segments of these chains to untangle from the melt.

Lamellar Thickness

A plot of lamellar thickness versus undercooling is shown in Figure 12. Note the rapid change in l for small changes in ΔT at the smaller undercoolings. At

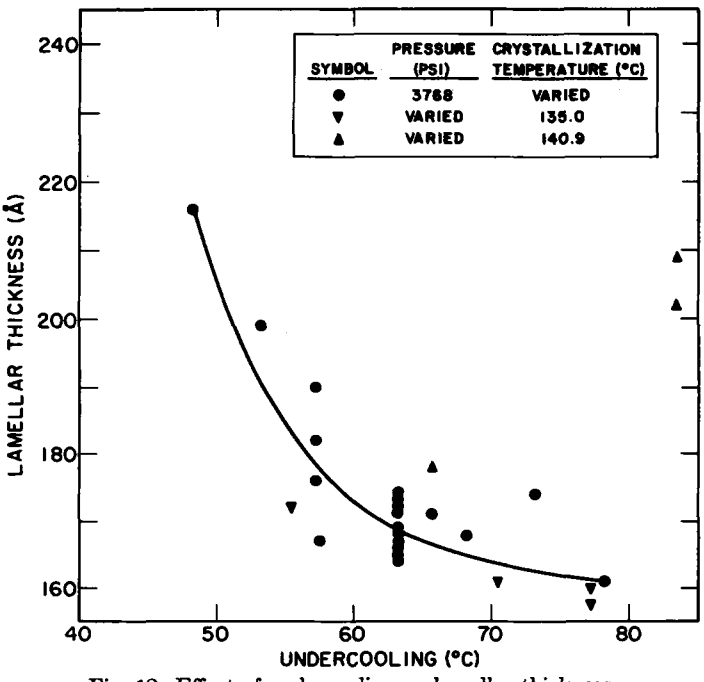

Fig. 12. Effect of undercooling on lamellar thickness.

higher undercoolings the curve begins to level off. Note also that the increase in l with decreasing undercooling contributes to the increase in density (i.e., per cent crystallinity) with decreasing undercooling. This is because an increase in l results in an increase of the ratio of crystalline lamellar volume to semiamorphous, lamellar fold plane surface.

High Undercooling Anomalies

Let us now turn our attention to the two samples crystallized at the highest undercooling (and pressure) employed in this study. As seen on Figure 10, these two samples exhibit the highest densities measured and lie in the direction opposite the trend of the rest of the data. X-Ray diffraction patterns for these samples show they contain α with only a trace amount of γ, a fact which is puzzling since γ is of greater density than α. This behavior is also unusual since high pressures have previously been believed to favor formation of γ in preference to α.[28]

In contrast, these samples have measured heats of fusion that lie slightly below the trend of the rest of the data shown on Figure 11. A possible explanation for this lies in the fact that these samples contain only a trace amount of γ while the remainder of the samples contain substantially more. Since γ is the more dense form, it is expected that its heat of fusion would be greater than α. Thus, at the same per cent crystallinity, a predominately α sample with only a trace amount of γ should have a measured heat of fusion slightly below that expected from a sample with a more substantial amount of γ.

Using the same reasoning discussed previously, comparison of heat of fusion and density data would seem to lead to the conclusion that these two samples have significantly less porosity than the remainder of the samples. It is not clear why such a large change should occur over such a small range of undercooling. Optical microscopy reveals no observable differences in void content between these two samples and the remainder of the samples crystallized at moderate to higher undercoolings. Thus the reasons for this behavior remain unresolved at this time.

As seen on Figure 12, lamellar thickness versus undercooling, the two highest undercooling samples again exhibit strikingly anomalous behavior. Again, the reasons for the rapid change in lamellar thickness over such a small range of undercooling remain unknown.

Application to Commercial Processing

The range of experimental variables employed in this study fit quite well with those that are expected in commercial injection molding processes. Typical commercial melt temperatures are on the order of 200° to 290°C,[29] the low end of which correlate well with the 190° to 220°C range employed here. Typical injection pressures range from 10,000 to 20,000 psi,[29] with mold pressures being on the order of 25–75% of these values,[30] in reasonable agreement with the pressures employed in this study.

Table II lists typical expected values of the variables investigated in this study for undercoolings of 50°, 65°, and 80°C. As mentioned earlier, an incremental increase in ΔT brought about by a crystallization temperature decrease is slightly more effective in inducing nucleation than is a pressure increase producing an identical incremental increase in ΔT. Thus, although values of nucleation

TABLE II
Summary of Typical Expected Values

ΔT, °C	Nucleation density,[a,b] mm^{-3}	Spherulite growth rate, μ/min	Time for 50% crystallization,[a] min	Spherulite diameter,[a,b] mm × 10^2	Lamellar thickness, Å	Density, g/cm^3	Density per cent crystallinity,[c] %	Heat of fusion, cal/g	Heat of fusion per cent crystallinity,[d] %
50	100	0.5	95	14	205	0.9143	77	−22.2	67
65	550	4	9	9.5	167	0.9118	74	−21.8	66
80	5000	9	3	4.5	161	0.9093	71	−21.4	65

[a] For moderate melt treatment.

[b] Values are approximate due to difference in pressure and crystallization temperature effects.

[c] Calculated ignoring the presence of γ and using the equation

$$\% \text{ crystallinity} = 100\left[\frac{\frac{1}{\rho_{RT}} - \frac{1}{\rho_a}}{\frac{1}{\rho_c} - \frac{1}{\rho_a}}\right]$$

where ρ_{RT} is the measured sample density, ρ_a is the amorphous density (0.850 g/cm^3),[23] and ρ_c is the α density (0.936 g/cm^3).[23]

[d] Calculated ignoring the presence of γ and using the equation

$$\% \text{ crystallinity} = 100\left[\frac{\Delta H_f}{\Delta H_f(100\%)}\right]$$

where ΔH_f is the measured heat of fusion and $\Delta H_f(100\%)$ is the heat of fusion of a 100% crystalline α sample (−33 cal/g).[20]

density and resultant spherulite diameter are strong functions of undercooling for a set melt treatment, they have an additional dependence on pressure and/or crystallization temperature. These two parameters, as well as the time for 50% crystallization, are also functions of melt history. However, spherulite growth rate, lamellar thickness, density, density per cent crystallinity, heat of fusion, and heat of fusion per cent crystallinity are unique functions of undercooling.

If it is desirable in a commercial process to decrease spherulite size in a controlled manner, the mold temperature can be decreased and/or the injection pressure increased to produce the trend shown in Table II. (Note, as mentioned previously, there are practical limitations to this. It is because of these practical limitations that nucleating agents find wide use, both to achieve optical clarity by producing a small spherulite size and to decrease cycle time by increasing crystallization kinetics.) A 30°C change in undercooling as shown in the table is equivalent to a pressure change of about 8900 psi. From Table II, a 30°C increase in undercooling from 50° to 80°C results in the spherulite diameter being decreased more than threefold. This is the result of greater nucleation density which is seen to increase about 50-fold between these undercooling limits. This increase in nucleation density, in combination with an 18-fold increase in spherulite growth rate, results in the 30-fold decrease in the time required for 50% crystallization. Additionally, note that lamellar thickness is decreased about 20%, while density per cent crystallinity decreases about 9% and heat of fusion per cent crystallinity about 3%.

While changes in spherulite diameter, density, density per cent crystallinity, heat of fusion, and heat of fusion per cent crystallinity are about linear with undercooling for the range of undercoolings employed, the other variables listed in Table II are not. Thus, the 15°C increase in undercooling achieved by going from 50° to 65°C produces a smaller incremental increase in both nucleation density and spherulite radial growth rate than the increase in undercooling in going from 65° to 80°C. However, the change on going from 50° to 65°C produces a greater incremental decrease in the time for 50% crystallization than does a change from 65° to 80°C. This latter result is probably due to the fact that heat flow considerations are beginning to become important at the 80°C undercooling.

Note that a decrease in spherulite size could also be accomplished by decreasing the melt temperature. This processing change would increase the nucleation density and result in a decrease in crystallization time, without affecting lamellar thickness or the other variables shown in Table II. For example, as shown by Figure 9, a switch from a moderate to mild melt treatment at 50°C undercooling reduces the spherulite diameter by about $^1/_3$, from 0.14 mm to 0.10 mm. This results in a roughly fourfold decrease in time for 50% crystallization, from about 95 min to about 20 min.

CONCLUSIONS

The Clausius-Clapeyron equation quite adequately combines crystallization temperature and pressure into one processing parameter, undercooling, defined as the difference between the melting temperature and the crystallization temperature. Undercooling thus calculated plays a critical role in determining the kinetics of crystallization as well as the resultant structure.

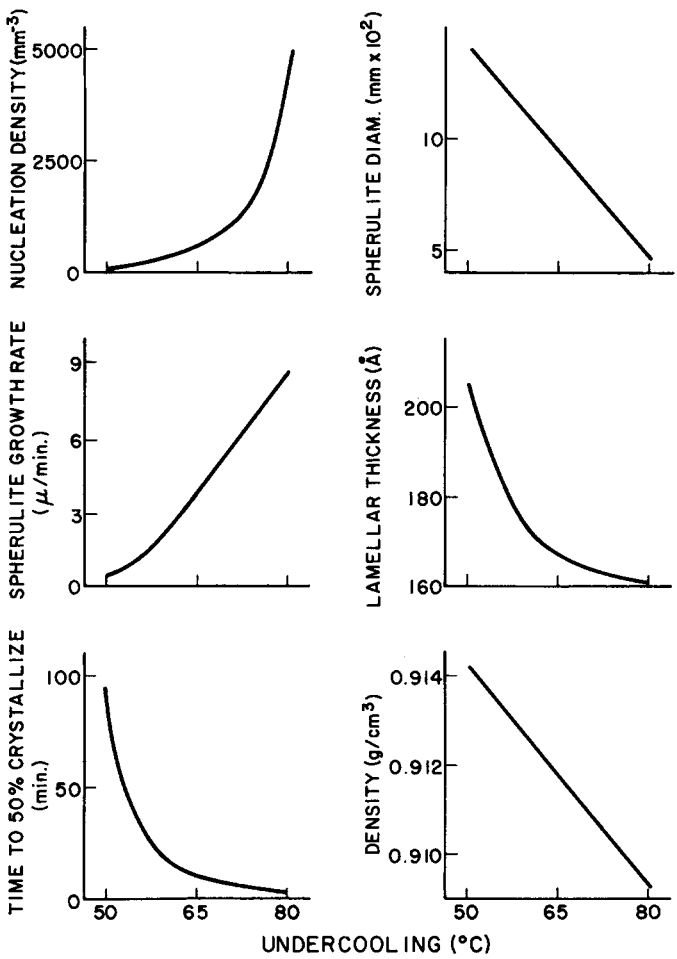

Fig. 13. Graphic summary of the effects of undercooling.

The effect of undercooling on crystallization kinetics and resultant structure are summarized in Figure 13. Increased undercooling results in increased nucleation density and thus decreased spherulite size. Changing undercooling from 50° to 80°C results in a 50-fold increase in nucleation density and a three-fold decrease in spherulite diameter. Increased pressure is not quite as effective in inducing nucleation as is predicted by the undercooling equation.

Increased undercooling also results in increased spherulite growth rate and decreased lamellar thickness, crystallization time, and per cent crystallinity. For example, increasing undercooling from 50° to 80°C results in a nearly 20-fold increase in spherulite growth rate, a 20-per cent decrease in lamellar thickness, a 30-fold decrease in time for 50% crystallization, and a small decrease in per cent crystallinity, reflected by a decrease in sample density.

The moderate to high undercoolings employed in this study are quite representative of conditions found in commercial injection-molding processes. Thus, the kinetic and structural trends found in this study should help explain those found in commercial processes.

Appendix I

List of Symbols

D	spherulite diameter
dh	incremental change in sample height
$\left(\frac{dh}{dt}\right)_{50\%}$	time rate of change of sample height at 50 mass-% transformed
dM	mass of polymer melt transformed from amorphous to semicrystalline state
$\left(\frac{dr}{dt}\right)_{50\%}$	spherulite radial growth rate at 50 mass-% transformed
dV	incremental change in volume due to transformation of mass dM from amorphous to semicrystalline state
h	sample height
h_{RT}	sample height at room temperature
l	lamellar thickness
M_0	sample mass
M_s	spherulite mass
N_v	nucleation density
P	pressure
P_0	reference pressure (3768 psi)
R	cylindrical mold radius (equal to sample radius)
r	spherulite radius
$r_{50\%}$	spherulite radius at 50 mass-% transformed
T_m	melt temperature
T_{mp}	equilibrium melting temperature (varied by pressure)
T^0_{mp}	equilibrium melting temperature at reference pressure of 3768 psi
T^∞_{mp}	melting temperature of lamella of infinite extent at atmospheric pressure
T'_{mp}	sample melting temperature measured at atmospheric pressure
T''_{mp}	sample melting temperature at reference pressure of 3768 psi
T_x	crystallization temperature
V_a	specific volume of amorphous melt
V_s	spherulite volume
V_{sc}	specific volume of semicrystalline polymer
ΔH_f	heat of fusion
ΔH_f (100%)	heat of fusion of 100% crystalline α
Δh	change of sample height due to thermal contraction on cooling from T_m to T_x
Δh_x	sample height change due to crystallization
ΔT	undercooling parameter, equal to T_{mp} minus T_x
ΔV_f	specific volume change on fusion
ρ_a	amorphous density
ρ_c	100% crystalline α density
ρ_{RT}	measured sample density at 23°C
ρ_{sc}	density of semicrystalline polymer

Appendix II

Calculation of Spherulite Radial Growth Rate

During the transformation we note a time rate of volume change of

$$\frac{dV}{dt} = \pi R^2 \left(\frac{dh}{dt}\right)$$

where R is the cylindrical mold or sample radius and dh/dt is the measured time rate of change of sample height. A volume change dV results from the transition of amorphous melt to semicrystalline polymer and, for an amount of mass dM transformed,

$$dV = dM(V_a - V_{sc})$$

where V_a is the specific volume of the amorphous melt and V_{sc} is that of the crystallized polymer at the temperature and pressure in question. Thus,

$$\frac{dM}{dt} = \left(\frac{1}{V_a - V_{sc}}\right)\frac{dV}{dt} = \left(\frac{1}{V_a - V_{sc}}\right)(\pi R^2)\left(\frac{dh}{dt}\right)$$

The total number of spherulites in the sample is simply

$$(N_v)(\text{volume of sample}) = (3/4D)^3(h_{RT}\pi R^2)$$

where h_{RT} is the sample height measured at room temperature and D is the spherulite diameter.

Thus, per spherulite, the amount of mass added per unit time is

$$\frac{dM_s}{dt} = \frac{\left(\frac{1}{V_a - V_{sc}}\right)(\pi R^2)\left(\frac{dh}{dt}\right)}{(3/4D)^3\,(h_{RT}\pi R^2)} = \frac{\left(\frac{1}{V_a - V_{sc}}\right)\left(\frac{dh}{dt}\right)}{(3/4D)^3\,(h_{RT})} \tag{A1}$$

Prior to impingement, the volume of a spherulite is

$$V_s = \frac{4\pi r^3}{3}$$

where r is the spherulite radius.

Thus, $dV_s = 4\pi r^2 dr$; and, since $dM_s = dV_s(\rho_{sc} = 1/V_{sc})$, it follows that

$$\frac{dM_s}{dt} = \frac{dV_s}{dt}\rho_{sc} = \rho_{sc}4\pi r^2\left(\frac{dr}{dt}\right). \tag{A2}$$

If we equate (A1) and (A2), we obtain

$$\frac{dr}{dt} = \frac{\left(\frac{1}{V_a - V_{sc}}\right)\left(\frac{dh}{dt}\right)}{(3/4D)^3\,(h_{RT})(\rho_{sc}4\pi r^2)}. \tag{A3}$$

We chose to determine the radial growth rate when 50 mass-% of the specimen has transformed because at this time all transients have disappeared from the dilatometric trace for most of the undercoolings employed. The total mass of the sample is $h_{RT}\pi R^2\rho_{RT}$, where ρ_{RT} is the sample density at 23°C. Thus, 50% of the mass is obviously half of this amount and occupies a volume of $(h_{RT}\pi R^2\rho_{RT}/2)(1/\rho_{sc})$. Thus, the volume per spherulite at 50 mass-% transformed is

$$\frac{\left(\frac{h_{RT}}{2}\right)\pi R^2(\rho_{RT}/\rho_{sc})}{(3/4D)^3(h_{RT})(\pi R^2)} = (4D/3)^3(1/2)(\rho_{RT}/\rho_{sc}).$$

This is simply equal to $(4/3)\pi r^3_{50\%}$, where $r_{50\%}$ is the spherulite radius after 50 mass-% of the sample has transformed. Thus,

$$r_{50\%} = \frac{4D}{3}\left[(3/8\pi)(\rho_{RT}/\rho_{sc})\right]^{1/3}. \tag{A4}$$

We also note that

$$V_a - V_{sc} = \frac{\text{total change in sample volume}}{\text{sample weight}} = \frac{\pi R^2 \Delta h_x}{\rho_{RT} h_{RT} \pi R^2} = \frac{\Delta h_x}{h_{RT} \rho_{RT}}. \tag{A5}$$

Substituting (A4) and (A5) in (A3) we obtain

$$\left(\frac{dr}{dt}\right)_{50\%} = \left(\frac{dh}{dt}\right)\left(\frac{D}{\Delta h_x}\right)\left(\frac{4(\rho_{RT}/\rho_{sc})^{1/3}}{(3)^{5/3}(\pi)^{1/3}}\right). \tag{A6}$$

If we now assume $(\rho_{RT}/\rho_{sc}) \simeq 1$ and note that because the cube root of this ratio is taken, it enhances the assumption, eq. (A6) becomes

$$\left(\frac{dr}{dt}\right)_{50\%} = \left(\frac{0.44D}{\Delta h_x}\right)\left(\frac{dh}{dt}\right)_{50\%}$$

which is the equation cited in the text.

Appendix III

Calculation of T^0_{mp}

The determination of T^0_{mp}, the equilibrium melting temperature at the reference pressure, requires a knowledge of how the melting temperature varies with crystallization temperature *at the reference pressure.* Note that eq. (3) in the text relates the DSC melting temperature T'_{mp}, measured at atmospheric pressure, to the crystallization temperature. This equation must be "corrected" to reflect the melting temperature that would be measured at the reference pressure, T''_{mp}. To do this, we make use of the Clausius-Clapeyron equation, which we now write in functional notation as

$$T'_{mp} = \left[\frac{\Delta V_f(P = 3768, T_x) T''_{mp}}{\Delta H_f(T_x)}\right] \Delta P + T''_{mp}$$

where T'_{mp} is given as a function of T_x by eq. (3), and $\Delta V_f(P = 3768, T_x)$ is the specific volume change on fusion at 3768 psi and the crystallization temperature; it is determined as a function of crystallization temperature by substitution of $P = 3768$ psi into eq. (1). $\Delta H_f(T_x)$ is given as a function of crystallization temperature by eq. (2). (Note that both ΔV_f and ΔH_f are for the whole polymer, not for just the crystalline portion. However, the ratio $\Delta V_f/\Delta H_f$, which appears in the Clausius-Clapeyron equation, is for just the crystalline portion.) ΔP is simply the pressure at which T'_{mp} is measured (0 psi gauge) less the pressure to which T''_{mp} is referred (3768 psi gauge). After eqs. (1), (2), and (3) and ΔP are substituted in the above equation, the solution of T''_{mp} as a function of T_x is straightforward. This relationship is then plotted as shown on Figure 2 and T^0_{mp} is determined as the temperature at which this line intersects the line $T''_{mp} = T_x$.

The authors are indebted to Dr. S. Pollack of Mellon Institute for performing the x-ray measurements cited in this study and for providing valuable advice on their interpretation. The authors also wish to thank Hercules, Incorporated for supplying the polymer used in this study.

One of the authors (J.H.R.) also gratefully acknowledges the fellowship support provided by the Ford Foundation, the International Nickel Company, and the National Science Foundation.

References

1. V. A. Kargin, T. I. Sogolova, and L. I. Nadareishvili, *Polym. Sci. USSR*, **6**, 1404 (1954).
2. H. W. Starkweather, Jr., G. E. Moore, J. E. Hansen, T. M. Roder, and R. E. Brooks, *J. Polym. Sci.*, **21**, 189 (1956).
3. C. F. Hammer, T. A. Koch, and J. F. Whitney, *J. Appl. Polym. Sci.*, **1**, 169 (1959).
4. S. M. Ohlberg, J. Roth, and R. A. V. Raff, *J. Appl. Polym. Sci.*, **1**, 114 (1959).

5. H. W. Starkweather, Jr., and R. E. Brooks, *J. Appl. Polym. Sci.*, **1**, 236 (1959).
6. J. van Schooten, H. van Hoorn, and J. Boerma, *Polymer*, **2**, 161 (1961).
7. R. S. Schotland, *Polym. Eng. Sci.*, **6**, 244 (1966).
8. S. W. Allison and I. M. Ward, *Brit. J. Appl. Phys.*, **18**, 1151 (1967).
9. E. R. Dixon and J. B. Jackson, *J. Mater. Sci.*, **3**, 464 (1968).
10. G. C. Oppenlander, *Science*, **159**, 1311 (1968).
11. L. A. Wood, N. Bekkedahl, and R. E. Gibson, *J. Chem. Phys.*, **13**, 475 (1945).
12. P. L. McGeer and H. C. Duss, *J. Chem. Phys.*, **20**, 1813 (1952).
13. L. R. Fortune and G. N. Malcolm, *J. Phys. Chem.*, **64**, 934 (1960).
14. E. Baer and J. L. Kardos, *J. Polym. Sci., A-3*, 2827 (1965).
15. G. M. Martin and L. Mandelkern, *J. Appl. Phys.*, **34**, 2312 (1963).
16. B. Wunderlich and T. Arakawa, *J. Polym. Sci., A-2*, 3697 (1964).
17. L. Mandelkern, N. L. Jain, and H. Kim, *J. Polym. Sci. A-2*, **6**, 165 (1968).
18. H. N. Beck and H. D. Ledbetter, *J. Appl. Polym. Sci.*, **9**, 2131 (1965).
19. J. H. Reinshagen and R. W. Dunlap, *J. Appl. Polym. Sci.*, **17**, 3619 (1973).
20. R. T. DeHoff and F. N. Rhines, *Quantitative Microscopy*, McGraw-Hill, New York, 1968, Chap. 7.
21. F. L. Binsbergen and B. G. M. DeLange, *Polymer*, **11**, 309 (1970).
22. J. J. B. P. Blais and R. St. John Manley, *J. Mac. Sci. Phys.*, **B1**, 525 (1967).
23. J. G. Fatou, *Eur. Polym. J.*, **7**, 1057 (1971).
24. F. Rybnikar, *Polymer*, **10**, 747 (1969).
25. H. D. Keith, *Kolloid-Z.*, **231**, 421 (1969).
26. G. Natta, P. Pino, P. Corradini, F. Danusso, E. Mantica, G. Mazzanti, and G. Moraglio, *J. Amer. Chem. Soc.*, **77**, 1708 (1955).
27. A. Turner Jones, J. M. Aizlewood, and D. R. Beckett, *Makromol. Chem.*, **75**, 134 (1964).
28. J. L. Kardos, A. W. Christiansen, and E. Baer, *J. Polym. Sci. A-2*, **4**, 777 (1964).
29. *Mod. Plast.*, **49(10A)**, 160 (1972).
30. G. D. Gilmore and R. S. Spencer, *Mod. Plast.*, **27(4)**, 143 (1950).

Received June 18, 1974
Revised September 24, 1974